Desalination and Water Treatment
www.deswater.com

doi: 10.1080/19443994.2015.1086701

57 (2016) 17557–17569
August

Taylor & Francis
Taylor & Francis Group

The influence of surface functionalization of activated carbon on dyes and metal ion removal from aqueous media

Amel Belayachi[a], Benaouda Bestani[a,*], Abdelaziz Bendraoua[b], Nouredine Benderdouche[a], Laurent Duclaux[c]

[a]*Laboratoire de Structure, Faculté des Sciences et de la Technologie, Elaboration et Application des matériaux Moléculaires (SEA2 M), Université Abdelhamid Ibn Badis, Mostaganem, Algeria, Tel. +213 790540538; Fax: +213 45206476; email: belayachiamel@gmail.com (A. Belayachi), Tel. +213 552329407; Fax: +213 45206476; email: bestanib@yahoo.fr (B. Bestani), Tel. +213 772618906; Fax: +213 45206476; email: benderdouchen@yahoo.fr (N. Benderdouche)*

[b]*Laboratoire de Synthèse organique, Physico-chimie, Biomolécules et Environnement (LSPBE), Département de chimie, Université des Sciences et de la Technologie d'Oran Mohamed Boudiaf, B.P 1505 Oran el M'naoueur, Oran, Algérie, Tel. +213 773616751; Fax: +213 41262108; email: bendraouas@yahoo.com*

[c]*Laboratoire de Chimie Moléculaire et Environnement (LCME), Université Savoie Mont Blanc, Chambéry F-73000, France, Tel./Fax: +33 0 479758805; email: laurent.duclaux@univ-savoie.fr*

Received 25 April 2015; Accepted 15 August 2015

ABSTRACT

Enhancement of the adsorptive properties of commercial activated carbons by simple surface modifications using chemical agents and their application to methylene blue, bemacid blue N-TF dyes, and nickel(II) ion removal from their aqueous solutions was the aim of this study. Impregnations in 10% KOH (MAC-K) for 24 h and concentrated H_2SO_4 (MAC-S) for 2 h, applied to Merck activated carbon, and NaOH (RHAC-N) with different strength applied to Riedel- de Haen activated carbon in order to functionalize and to modify their surfaces were investigated. These treatments were found to increase the adsorption capacity of the considered pollutants significantly relative to their untreated state of up to 250.00 mg/g for methylene blue, 11.47 mg/g for nickel(II) ions, and 312.00 mg/g for bemacid blue ET-L by MAC-K, MAC-S, and RHAC-N, respectively. Three well-known model equations namely Langmuir, Freundlich, and Temkin were used to analyze the adsorption equilibrium data. Parameters influencing adsorption capacity such as contact time, adsorbent dosage, pH, and temperature were studied. FT-IR and DRX analysis were performed for chemical functionalities; pH_{zpc}, methylene blue accessible area, iodine number, and morphological analysis by scanning electron microscopy determination were also performed to characterize the prepared adsorbents. Adsorption kinetics was found to comply with the pseudo-second-order with a good correlation factor ($R^2 = 0.99$) and with intra-particle diffusion as the rate-determining steps. This study showed that surface functionalization of activated carbon could prove to be a very useful method in removing toxic substances from wastewater and the environment.

Keywords: Activated carbon; Surface modification; Functionalization; Adsorption; Nickel(II) ions; Dyes

*Corresponding author.

1. Introduction

The growth of the industrial activity in the last decades had largely contributed to the environment contamination by different pollutants such as heavy metals and all kind of organic substances. Thus, becoming a serious problem, even with low concentrations, these contaminants constitute a major threat [1,2]. In particular, dyes from textile industries are often discharged in the environment in the form of colored wastewater without any prior treatment representing then, an important class of pollutants affecting human health by damaging vital organs and also can be toxic to aquatic life [3–6]. They are often used in excess to improve the dyeing process leading to water rejection strongly concentrated in dyes of which the reliable biodegradability makes the biological treatments not easily applicable [7].

In this study, one heavy metal and two dyes are chosen to be removed from aqueous solutions by adsorption using functionalized commercial activated carbons. Firstly, nickel as heavy metal is a compound that occurs in the environment only at very low levels. Foodstuffs naturally contain small amounts of nickel, while chocolate and fats are known to contain high quantities. Nickel uptake increases when people eat large quantities of vegetables from polluted soils. Plants are known to accumulate nickel and as a result the nickel uptake from vegetables will be eminent. Nickel is released into the air by power plants and trash incinerators from which humans may be exposed to this toxic metal by breathing air.

Secondly, methylene blue as basic aniline dye is a heterocyclic aromatic chemical compound. It has many uses in a variety of fields such as chemistry, biology, and aquaculture. In the latter, it is used as a treatment for fungal infections. Methylene blue is also very effective when used as part of a "medicated fish bath" for treatment of ammonia, nitrite, and as an antidote for cyanide poisoning and a bacteriological stain.

Finally, bemacid blue N-TF is an acid dyestuff chemically stable used for the textile finishing. Exposure to decomposition products may be hazardous to health with irritant effects.

It is also harmful and may cause long-term adverse effects in the aquatic environment. To straighten legislation, it is desirable to remove these pollutants among others from effluents before their discharge in nature. Many conventional methods were used for toxic pollutants removal from wastewater, but they are limited to a variety of chemicals for technical reasons and high cost of exploitation or may not be capable of treating large volumes of effluent without the risk of clogging, e.g. membrane filtration [8–12].

Nowadays, the use of solid materials for these pollutants removal is widely spreading. Among these materials, activated carbons have been widely used as adsorbents and catalyst supports due to their properties which determine their applications such as high surface area, large pore volume, and chemical-modifiable surface [13]. The adsorption efficiency of carbons to remove one type of contaminant is strongly dependent on their surface chemical features. Therefore, materials production by surface modification is of great interest for specific applications. Many oxidants such as concentrated HNO_3, H_2SO_4, NaOH, $KMnO_4$, and H_2O_2 have been extensively used for commercial activated carbons functionalization by impregnation [14–17]. The oxidizing agent solution, its concentration, and pH influence strongly the surface structure of the solid, making it then a good adsorbent.

In this work, two activated carbons commercially available were chemically modified by introducing new functional groups on their surfaces in order to enhance their adsorptive properties and their application to remove efficiently the considered pollutants from their aqueous media.

2. Materials and methods

2.1. Adsorbents and solutions preparations

Simple treatments using potassium hydroxide (10%, 24 h, 25˚C) and sulfuric acid (96%, 2 h, 80˚C) were applied to functionalize the surface and to modify the structure of Merck activated carbon in order to eliminate methylene blue and nickel(II) from aqueous solutions, respectively, while NaOH solutions with different concentrations were used to functionalize Riedel- de Haen activated carbon for bemacid blue N-TF dye removal. The obtained samples were washed several times with distilled water and dried overnight at 100˚C. Then grinded using Crosschop Vierzen grinder and sieved to obtain particle diameter lower than 71 μm.

Stock solutions with known concentrations were prepared according to standard procedure by dissolving the required amount of methylene blue, bemacid blue N-TF, and hydrated nickel sulfate separately in distilled water. Successive dilutions were used to obtain working solutions of the desired concentrations. Iodine standard solutions (0.1 ± 0.1 N) were prepared from sublimed iodine dissolved in potassium iodide and titrated with (0.1 ± 0.1 N) sodium thiosulfate which was standardized with chemically pure potassium iodate. Table 1 summarizes some important characteristics of the studied dyes and nickel(II) ions.

Table 1
Chemical characteristics of adsorbed substances

	Methylene blue	Bemacid blue N-TF	Nickel
Molecular formula	$C_{16}H_{18}ClN_3S{\cdot}3H_2O$	$C_{31}H_{26}N_3NaO_6S$	$NiSO_4{\cdot}6H_2O$
Molecular weight (g mol^{-1})	373.90	591.65	262.85
Maximum wavelength (λ_{max})[a]	665	602	465
Supplier	Merck	Bezema	Merck
CAS number	7,220-79-3	67,827-60-5	10,101-97-0
Water solubility (g/L)	44	80 at 80°C	850 at 20°C

[a]Experimentally obtained values.

2.2. Prepared samples characterization

Determination of the surface area accessible to methylene blue and iodine, morphological analysis using SEM, pH of zero point charge (pH_{PZC}), and the determination of surface functional groups using IRFT were performed to characterize some selected samples.

In order to know the adsorption capacities of the prepared samples, one must evaluate their physicochemical characteristics. In this study, characterization of the prepared samples was mainly focused on surface area determination. By comparing the adsorption characteristics toward Iodine number, methylene blue index, and phenol index, additional information was obtained.

Iodine number is a parameter widely used for activated carbon testing for its simplicity and a rapid assessment of adsorbent quality. It gives an estimate of its surface area and porosity. It is defined as the quantity in milligrams of iodine adsorbed by one gram of material when the iodine residual concentration of the filtrate is 0.02 ± 0.01 N according to ASTM D4607 standard method [18], which is based on a three-point isotherm. A standard iodine solution (0.1 ± 0.1 N) is treated with three different weights of adsorbent. The sample is treated with 10.0 ± 0.1 mL of 5% (V/V) HCl. The mixture is boiled for 30 s and then cooled at room temperature. 100.0 ± 0.1 mL of 0.1 ± 0.1 N iodine solution is immediately added to the mixture and stirred for 30 s. The solution is then filtered and 50.0 ± 0.1 mL of the filtrate is titrated with 0.1 ± 0.1 N sodium thiosulphate solution using thyodene (or starch) as an indicator. The amount of iodine adsorbed per gram of adsorbent is plotted against the residual iodine concentration, using logarithmic axes. If the residual iodine concentration is not within the range (0.008–0.04 N), the procedure is repeated using different carbon masses for each isotherm point. A regression analysis is applied to the three points and the iodine number is calculated as the amount adsorbed at a residual iodine concentration of 0.02 ± 0.01 N.

Methylene blue is a typical dye used to calculate the accessible surface of sorbents to large molecules. The available surface with methylene blue is calculated by the following equation:

$$S_{MB} = \frac{b.N.S}{M} \quad (1)$$

with S_{MB} is the surface area ($m^2\ g^{-1}$), b is maximum adsorption capacity (mg g^{-1}) based on a monolayer coverage (determined from the Langmuir model), N is Avogadro's number ($6.023 \times 10^{23}\ mol^{-1}$), S is the surface occupied by a molecule of methylene blue (taken as 119 $Å^2$), and M is the molecular weight of methylene blue (319.86 g mol^{-1}).

Methylene blue adsorption is often used to characterize the activated carbons mesoporosity, particularly those with large molecules using the method reported by Bestani et al. and Ouldmoumna et al. [19,20].

In order to monitor the textural development and porosity of the prepared activated carbons, scanning electron microscopy (SEM) was used. Identification of the principal functional groups present on adsorbents' surface was obtained using FTIR spectroscopy analysis (Perkin-Elmer spectrometer employing KBr samples).

pH is one of the most influential variables in the adsorption from solution, since this parameter can change the sign (or presence) of charges onto the adsorbate, the predominant charge (positive or negative) on activated carbon surface depends on the acidic or basic character of the adsorbent. Therefore, it is important to study the presence of acidic or basic functional groups on activated carbons. A general measurement of the carbon's acidity/basicity is the point of zero charge (PZC) at which the surface charge density is zero. It is usually determined in relation to dissolution pH: the pH of the solution at equilibrium with a solid when the later exhibits zero net electrical

charge on the surface. pH_{zpc} was determined as follows: 50.0 ± 0.1 mL of a 0.01 ± 0.01 M aqueous solution of NaCl was placed in each of a series of stoppered conical flasks. The pH of the solution in each flask was adjusted (from 2 to12) using 0.01 ± 0.01 M HCl or 0.01 M NaOH, respectively, following which 0.15 ± 0.01 g of activated carbon was added to each flask and the resulting suspensions stirred for 48 h then the final pH value was measured.

2.3. Pollutants adsorption

A completely mixed batch reactor technique for the adsorption experiments for each one of methylene blue, bemacid blue N-TF (dyes), and metal ion (Ni^{2+}) onto the functionalized activated carbon samples was conducted as a function of the adsorbent dosage (2–20 mg/L range), contact time (30–480 min range), and pH (2–12 range) in a series of capped 200.0 ± 0.1 mL Erlenmeyer flasks at ambient temperature. For such sorption studies, a 25.0 ± 0.1 mL volume of a pollutant solution of known initial concentration was mixed with a known amount of adsorbent. The adsorbents prepared, namely, MAC-K, MAC-S and RHAC-N, were used, respectively, to remove methylene blue, nickel(II) ions, and bemacid blue ET-L from their aqueous solutions.

The resulting suspension was then agitated magnetically at a constant speed of 150 rpm until equilibrium is reached. The time necessary to attain equilibrium has been ascertained from previous kinetic experiments. After the adsorption process had occurred, the resulting solution in each flask was centrifuged at 4,000 rpm and the supernatant analyzed using a UV–visible 2,121 Optizen spectrophotometer at maximum wavelength values shown in Table 1. Some solutions were diluted as required so that their absorbance remained within the linear calibration range according to Beer-Lambert law. Experiments were carried out in triplicate at room temperature. The equilibrium adsorption capacities (q_e) at different pollutant concentrations were determined according to mass balance given by the following relationship:

$$q_e = \frac{(C_0 - C_{eq})}{m} V \quad (2)$$

where C_0 is the initial dye concentration (mg/L), C_{eq} is the equilibrium dye concentration (mg/L), V is the volume of the liquid phase (mL), and m is the mass of the activated carbon sample (mg).

3. Results and discussions

3.1. Functionalized samples characterization

3.1.1. FTIR analysis

FTIR analyses were performed for some samples (Riedel-de Haën activated carbon) using KBr disk in order to determine the functional groups responsible for adsorbate uptakes. The chemical activation by NaOH induces the appearance of new functional groups, which transform its surface structure. Analysis of the measured IR spectra (not shown) show a broad of large bands at 3,855–3,736 cm^{-1}, medium bands at 3,600, and 3,372 cm^{-1} due to bonded and free O–H vibration, respectively. The two peaks observed at 1,768 and 1,717 cm^{-1} correspond to the vibrations of the carbonyl group (which may belong from carboxyl groups). The peak observed at 1,530 cm^{-1} suggests the existence in carboxylate ions. The peaks at 1,174 and 986 cm^{-1}, may be assigned to the vibrations of the C–O–C bonds in the carboxylic acids and esters. Oxygen-containing groups present on the activated carbon surface may affect both dyes and metal ions adsorption through complex electron donor–receiver interactions.

3.1.2. Microporous and mesoporous available areas determination

As shown in Table 2, iodine numbers of functionalized carbons slightly decrease (4.5% for MAC-K and 6.3% for MAC-S) compared to the nontreated commercial Merck-AC. These decreases can be explained by the increase of functional groups on carbon surface during treatments by oxidizing agents such as KOH, H_2SO_4, and H_3PO_4 … which lead to the decrease of existing micropores [4]. On the other hand, there is an increase in RHAC-N iodine number. This can be explained by the increasing number of micropores on the activated carbon surface. The phenol index representing the activated carbon macroporosity decreases by 50 and 76% during treatments by KOH and H_2SO_4, respectively, and may become mesoporous, microporous, or a combination of both as shown in Table 2. The accessible surface of the prepared adsorbents shows that the MAC-K is mainly mesoporous as shown by the methylene blue index compared to the nonfunctionalized Merck-AC.

3.1.3. Morphology

The SEM images of the three biosorbents prepared show relatively heterogeneous porous surfaces as shown in Fig. 1. The SEM images of the surfaces indi-

Table 2
Chemical characteristics of adsorbed substances

Adsorbents	Iodine number	Phenol index	Methylene blue index
Merck-AC	828.00	19.26	543.40
MAC-K	791.00	8.78	611.91
MAC-S	776.00	4.67	407.99
RHAC-N	918.11		339.00
Riedel de Haën-AC	951.91		546.50

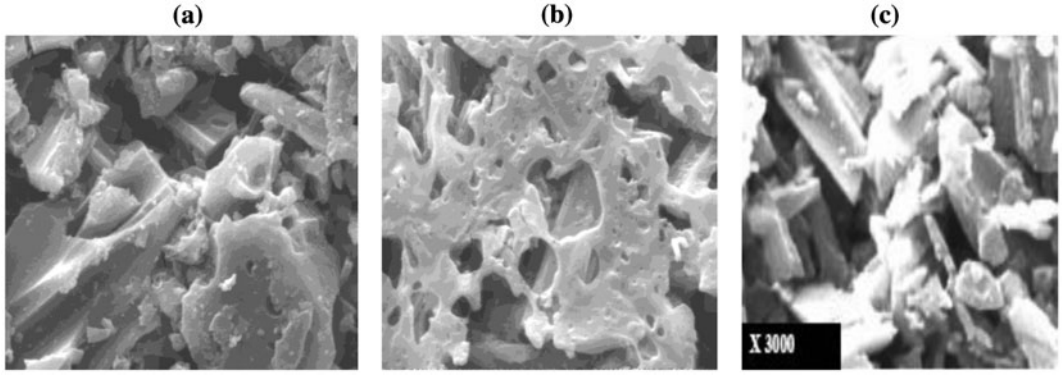

Fig. 1. SEM micrograph of the functionalized samples studied: (a) MAC-S, (b) MAC-K, and (c) RHAC-N.

cate that the particles were mainly arranged in layer-like structure.

The SEM images show that the prepared samples exhibit a porous and irregular surface with higher specific surface as determined by the iodine number since 1 mg of iodine adsorbed per gram of carbon represents approximatively a specific surface of 1 m^2/g [21]. In the case of sulfuric acid treatment, the porous structure of treated Merck activated carbon is less important than the untreated one. This may be due to pore destruction at higher concentrations of the acidic media.

3.1.4. Zero point of charge determination (pH_{zpc})

Fig. 2 shows the difference between the initial and final pH values ($\Delta pH = pH_i - pH_f$) plotted against (pH_i). For the case of MAC-K, the point of intersection of the resulting curve with the abscissa shown in Fig. 2, at which $\Delta pH = 0$, gave the PZC values [22–24].

Sulfuric acid treatments increase acidic functional groups. This increase has a slight effect on MAC-S' pH_{zpc} from 6.45 to 6.20 increasing then Ni ions adsorption capacity. At $pH < pH_{zpc}$, there is a repulsion between the carbon surface and Ni ions since they are both positively charged indicating a decrease in nickel(II) uptake. At $pH > pH_{zpc}$, there is an attraction between the negatively charged carbon surface and Ni ions increasing then the adsorption capacity.

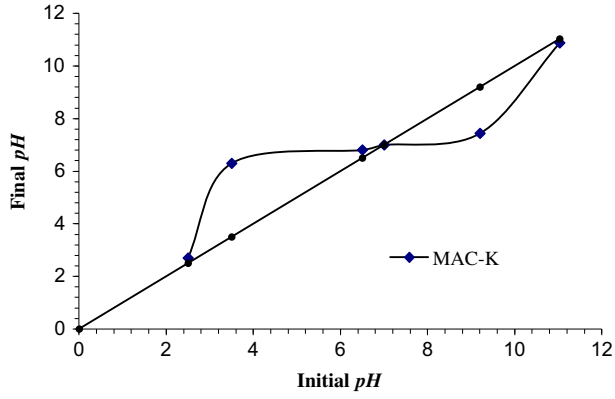

Fig. 2. Graphical representation of pH_{zpc} MAC-K adsorbent.

3.2. Parameters influencing adsorption

3.2.1. Equilibrium time determination

Depending on the adsorption type, longer contact time is required to attain equilibrium when the adsorption is of chemical nature resulting in a strong

binding of the adsorbate with the adsorbent. However, in physical adsorption, most of the adsorbate species are adsorbed on the interface within a short interval of contact time. In this study, experiments were carried out at optimum adsorbent dosage of methylene blue (8 g/L), Ni^{2+} (16 g/L), and bemacid blue (8 g/L). A 25.0 ± 0.1 mL solution of known initial concentration of the considered pollutants were mixed separately with an optimum adsorbent dosage of carbon determined previously and agitated at different time intervals ranging from 30 to 480 min at room temperature. The percentage removal was determined as:

$$\%\,\text{Removal} = \left(\frac{C_{\text{initial}}\,C_{\text{equilibrium}}}{C_{\text{initial}}}\right)100 \quad (3)$$

Fig. 3 shows the graphically plotted results of the % removal vs. time in which equilibrium time was reached after a contact time of 3 h for Ni^{2+} onto MAC-S and Merck-AC. It may be noted that 60% removal of Ni^{2+} onto MAC-S is obtained after 2 h of contact time and reaches a maximum of 70% after 3 h and stay stable for up to 6 h of agitation which means that equilibrium has been reached.

Fig. 3 shows that 3 h contact time was largely sufficient to almost completely remove methylene blue from aqueous solution by MAC-K (99%) in comparison with untreated AC (79%). Similar results have been obtained for the same concentration range, while a longer time (24 h) is obtained for higher concentrations [25]. It can be seen that the % removal increases with increasing contact time until equilibrium is reached.

The same figure shows that about 90% of the bemacid blue ET-L was removed within one hour by the RHAC-N material while it took two hours to reach equilibrium with 99% removal corresponding to a capacity of 189 mg/g. It has been reported that the removal efficiency reached 77% for bemacid blue after 4 h using fly ash [26].

3.2.2. pH effect on pollutants adsorption

It is well known that the pH of the adsorption medium is a critical parameter affecting the whole adsorption process, particularly the dye uptake [22,27].

However, the surface charge of the adsorbent type can be modified by the pH of the external solutions [28,29]. To determine the optimum pH conditions for the considered dyes and metal ion onto the chosen adsorbents, initial pH of the solution of known volume and fixed initial concentration was varied from 2 to 12 by adding either dilute NaOH or HCl solutions. Then a certain volume of this solution was placed in a flask to which a certain amount of adsorbent (dose determined previously) was added and the mixture was agitated then filtered and the final concentration of the considered pollutant determined by spectrophotometry. The data are presented in Fig. 4, which indicates that there was no major effects even at high pH values in methylene blue uptake onto the MAC-K adsorbent. In this case, no pH adjustment was needed for methylene blue adsorption tests. A significant increase in respective adsorption capacities of Ni^{++} and bemacid blue onto MAC-S and RHAC-N was observed with pH up to a certain value, then a decrease was noted at higher pH values. This decrease in adsorption capacity is due may be to high concentration of OH^- ions (basic environment) competing with the considered molecules (cationic) for the avail-

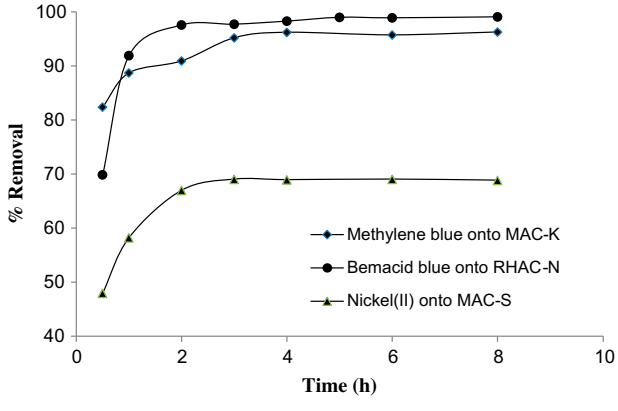

Fig. 3. % removal of the considered pollutants by the prepared samples.

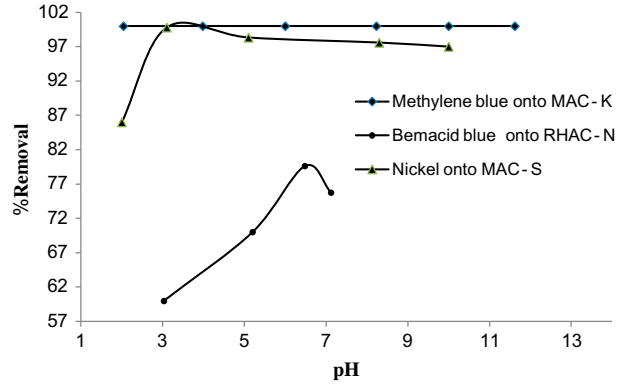

Fig. 4. pH effect on Ni^{2+} uptake onto MAC-S and MAC.

able sites which do not favor an attraction between both adsorbent surface and the pollutants and also the formation of nickel hydroxide. Similar adsorption behavior with variation in solution pH has been reported in the literature [23].

From the Fig. 4, maximum Ni^{2+} ions uptake was observed at pH values of 6.48 ± 0.01 and 5.50 ± 0.01 for MAC-S and Merck AC, respectively. At low pH values, there is a decrease in Ni^{2+} ions uptake; this is due to the excessive protonation (presence of H^+) competing with metal ions (acid environment) [30–32].

3.2.3. Adsorbent dose effect on adsorption

Carbon dose is usually used to predict the treatment cost of an adsorbent per unit of dye or metal ion solution and to determine equilibrium between the sorbent and the sorbate of a system. The adsorption dependence of methylene blue, bemacid blue, and Ni^{2+} on adsorbents dosage was studied by varying the amount of MAC-K, MAC-S, and RHAC-N within the range 2–24 mg/L maintaining all other experimental parameters constant. As shown in Fig. 5, the maximum uptake was attained at an adsorbent dosage of 16 g/L for Ni^{2+} (74% removal), 8 g/L for methylene blue (>99% removal), and 4 g/L for bemacid blue (99% removal) by the MAC-S, Mac-K, and RHAC-N adsorbents, respectively. Increasing adsorbent dosage can attribute to the availability of a greater number of adsorption sites. We note that at higher carbon dosage, there is a slight decrease in the adsorption capacity of the three pollutants. This is may be due to the overlapping of adsorption sites due to overcrowding of adsorbent particles as reported in the literature [33].

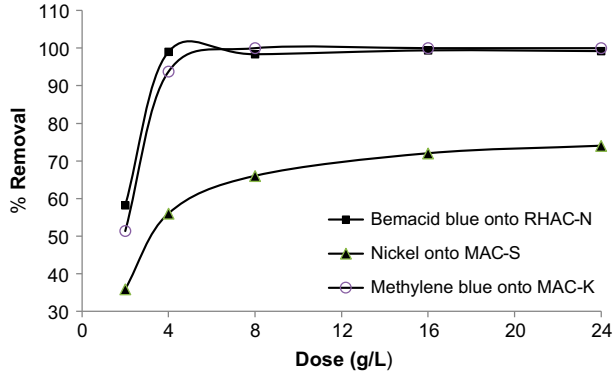

Fig. 5. Dose effect on dyes and metal ion adsorption by functionalized carbons.

3.3. Adsorption isotherms

The plots of solid phase against liquid phase concentrations can be used to describe the adsorbate–adsorbent interactions in order to depict the equilibrium adsorption isotherm graphically [24]. Single well-known component adsorption isotherms equations have been tested in the present study, namely Langmuir, Freundlich, and Temkin. These isotherms [34,35] are represented by the following linearized forms:

$$\text{Langmuir isotherm:} \quad \frac{C_{eq}}{q_e} = \frac{1}{Kb} + \frac{1}{b} C_{eq} \tag{4}$$

where q_e is amount of solute adsorbed per unit weight of adsorbent (mg/g). C_{eq} is the concentration of solute remaining in solution at equilibrium (mg/L), b (mg/g) is the maximum adsorption capacity corresponding to complete monolayer coverage, and K is a constant related to the energy or net enthalpy. b and K are estimated from the linear relationship obtained by plotting specific adsorption (C_{eq}/q_e) against the equilibrium concentration (C_{eq}) as shown in Fig. 6, with the correlation coefficient ($R^2 = 0.99$) for all three pollutants which confirms the applicability of the Langmuir model indicating the homogeneous nature of the considered adsorbent, i.e. there is equal adsorption activation energy for each dye molecules or metal ion. The data also demonstrate the formation of monolayer coverage of dye molecules and metal ions at the outer surface of the adsorbent studied. Obtained from the Langmuir model, the maximum monolayer capacities b for the adsorption of methylene blue, Ni^{2+} and bemacid blue onto MAC-K, MAC-S, and RHAC-N, respectively, were 250, 11.47, and 312.5 mg/g at ambient temperature as mentioned in Table 3. The significant enhancements of 12% for methylene blue, 82% for Ni^{2+}, and 25% for bemacid blue obtained by the chemical treatments are clear evidence that the functionalization (activation) improves the adsorptive ability of commercial AC compared to untreated ones. Values are compared to some maximum capacities using other adsorbents obtained from the literature as shown in Table 4.

$$\text{Freundlich isotherm:} \quad \log q_e = \log k_f + \frac{1}{n} \log C_{eq} \tag{5}$$

Equilibrium data for the adsorption of methylene blue, Ni^{2+} ions, and bemacid blue were also analyzed using the Freundlich model represented by Eq. (5). Where k_f and n are the Freundlich constants related to adsorption capacity and adsorption intensity that can be obtained from the intercept and slope of log q_e vs. log

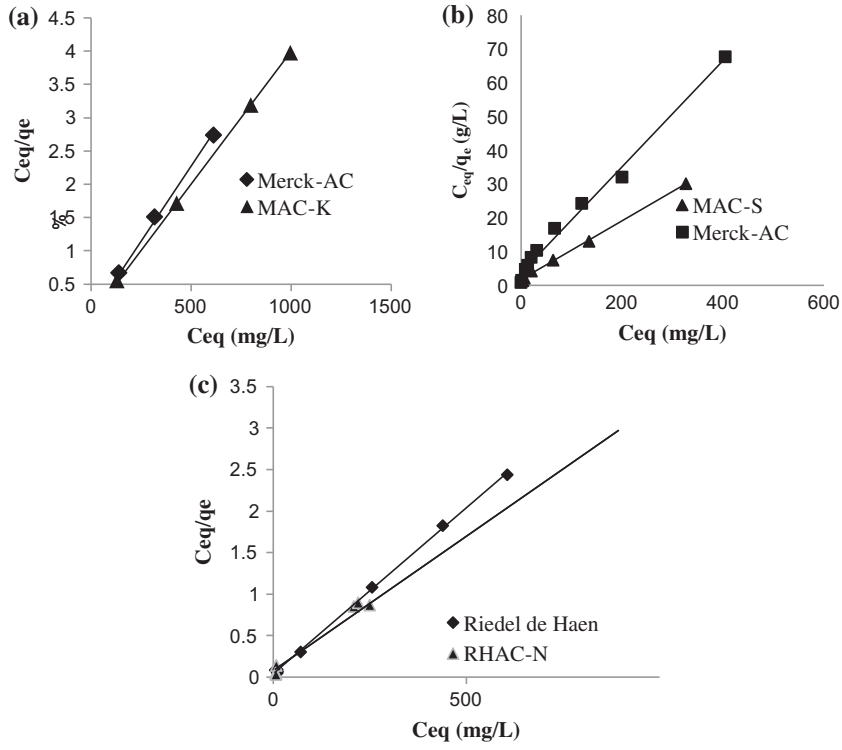

Fig. 6. Plots for Langmuir adsorption isotherms of (a) Methylene blue, (b) Nickel, and (c) Bemacid blue on the modified activated carbons.

Table 3
Langmuir, Freundlich, and Temkin parameters for Ni^{2+}, methylene blue, and bemacid blue ET-L removal by the modified adsorbents and the commercial one

		Isotherm models								
		Langmuir			Freundlich			Temkin		
Adsorbents	Adsorbates	b (mg/g)	k (L/mg)	R^2	n	k_f (mg/g)	R^2	b_T (kJ/mol)	ln K_T	R^2
Merck-AC[a]	Ni^{+2}	6.30	0.05	0.99	2.80	0.87	0.97	2.70	0.43	0.91
MAC-S		11.47	0.05	0 .99	2.1 3	1.03	0.93	1.33	0.04	0.95
Merck-AC[a]	Methylene blue	222.20	0.26	0.99	9.02	118.40	0.83	0.16	8.54	0.92
MAC-K		250.00	0.43	0 .99	9.56	135.90	0.75	0.15	9.26	0.87
Riedel-Haen AC[a]	Bemacid blue ET-L	250.00	0.10	0.99	0.23	68.77	0.61	0.08	1.86	0.73
RHAC-N		312.50	0.04	0.99	4.70	76.12	0.62	0.68	1.65	0.79

[a]Nontreated activated carbon.

C_{eq} plot. The Freundlich parameters are shown in Table 3.

Fig. 7 represents the plot of ln q_e vs. ln C_{eq}, which is not a straight line, indicating the nonapplicability of the Freundlich equation for the adsorption of both dyes, while it is more representative for metal ions adsorption with correlation coefficients ($R^2 > 0.99$) indicating that the experimental data can be fitted well to this model and the adsorption process is favorable ($n > 1$). Compared to Langmuir model, the Freundlich isotherm appears to be less applicable. Similar results were reported during the adsorption of yellow bemacid dye [36].

The Temkin adsorption isotherm model was chosen to evaluate the adsorption potentials of the adsorbent for adsorbates. It assumes that the heat of adsorption (b_h) of all the molecules in the layer decreases linearly with coverage due to adsorbate–adsorbate repulsions and the adsorption is a uniform distribution of maximum binding energy (K_T).

Table 4
Adsorption capacities of methylene blue, Ni^{2+}, and bemacid blue on various adsorbents prepared from raw materials

Pollutant	Adsorbent	Max. capacity (mg/g)	Refs.
Methylene blue	Eucalyptus globulus	250.00	[20]
	Salsola vermiculata	130.00	[19]
	Functionalized AC	250.00	This study
	Date pits	259.25	[37]
Nickel(II)	Coir pitch	15.95	[38]
	Brewer's yeast	5.34	[39]
	Functionalized AC	11.47	This study
	Orange peel	62.89	[40]
Bemacid blue	Orange peel	31.39	[41]
	Functionalized AC	321.50	This study

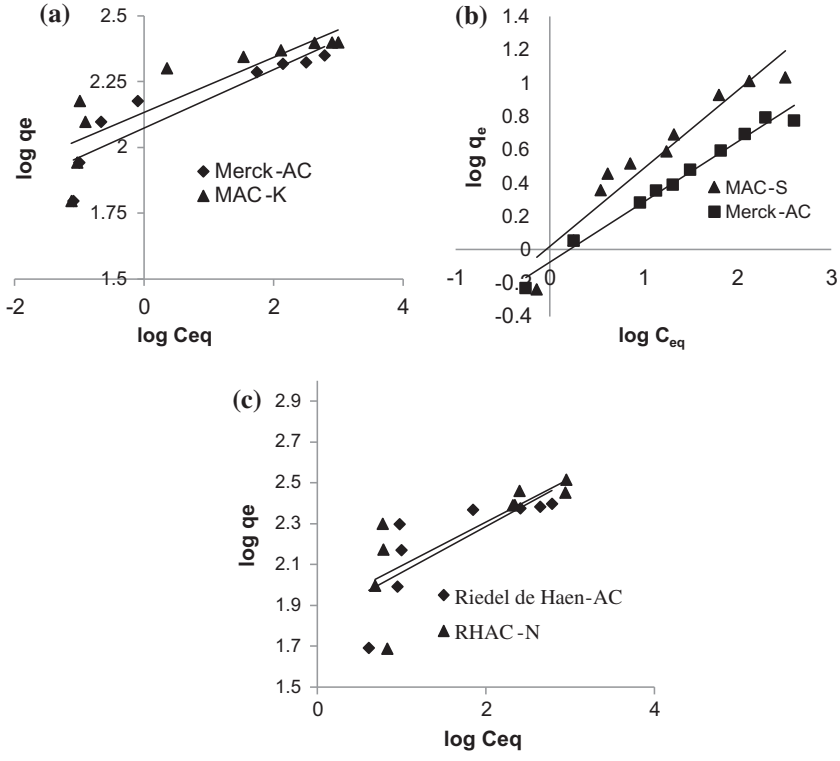

Fig. 7. Plots for Freundlich adsorption isotherms of (a) Methylene blue, (b) Nickel, and (c) Bemacid blue on the modified activated carbons.

The Temkin isotherm is represented by the following equation:

$$q_e = B \ln K_T + B \ln C_{eq} \quad (6)$$

where q_e (mg/g) and C_{eq} (mg/L) are the amounts of adsorbed dye per unit weight of adsorbent and unadsorbed dye concentration in solution at equilibrium, respectively, and $B = (RT)/b_h$. T the absolute temperature (°K) and R is the universal gas constant (8.314 J/mol K). The constant b_h is related to the heat of sorption (J/mol) and K_T is the equilibrium binding constant.

The Temkin adsorption potential, K_T, of MAC-S for Ni(II), MAC-K for methylene blue, and bemacid blue ET-L are summarized in Table 3. Higher values of K_T for both dyes indicate strong adsorbate–adsorbent interaction in agreement with the obtained values of

adsorption capacities of 250 mg/g (methylene blue) and 312.5 mg/g (bemacid blue ET-L) by MAC-K and RHAC-N, respectively. Lower values of K_T for Ni ions indicate a lower MAC-S-metal ion potential for Ni(II) probably due to its small ionic radius and charge. The Temkin constant, b_T, related to heat of sorption for the three pollutants were 1.33 kJ/mol, 0.15 k J/mol, and 0.07 kJ/mol for Ni^{2+}, methylene blue, and bemacid blue ET-L, respectively (as computed from Fig. 8 and shown in Table 3).

3.4. Adsorption kinetics

Three models namely pseudo-first-order, pseudo-second-order, and intra-particle [42–44] were used in this study to evaluate the kinetic mechanism of the adsorption process and to test the experimental data using two different concentrations for each adsorbate. These models were tested and their validity was verified by linear equation plot analysis. The linearized forms of the three models are expressed as follow:

3.4.1. Pseudo-first-order model

$$\log(q_e - q_t) = \log q_{e,1} - \frac{k_1}{2.303}\, t \tag{7}$$

where q_e and q_t, are the sorption capacity at equilibrium and at time t, respectively (mg/g). k_1 is the rate constant of pseudo-first-order adsorption. k_1 and q_e are determined from the slope and intercept of log ($q_e - q_t$) vs. t plot, respectively.

3.4.2. Pseudo-second-order model

$$\frac{t}{q_t} = \frac{1}{k_2 q_{e,2}^2} + \frac{1}{q_e} t \tag{8}$$

where k_2 is the pseudo-second-order overall rate constant (mg g^{-1} min^{-1}). $k_2 q_{e,2}^2$ can be assumed as the initial adsorption rate as t goes to zero. The linearity of t/q_t vs. t plots implies that the second-order kinetics is representative and k_2 and $q_{e,2}$ are calculated from the slope and the intercept, respectively (Fig. 6).

3.4.3. Intra-particle diffusion

It is well known that the transport rate is influenced by the adsorbent's structure and its interaction with the diffusion adsorbate. In order to describe the adsorption process occurring on solid phase, the intra-particle diffusion model represented by Eq. (9) has

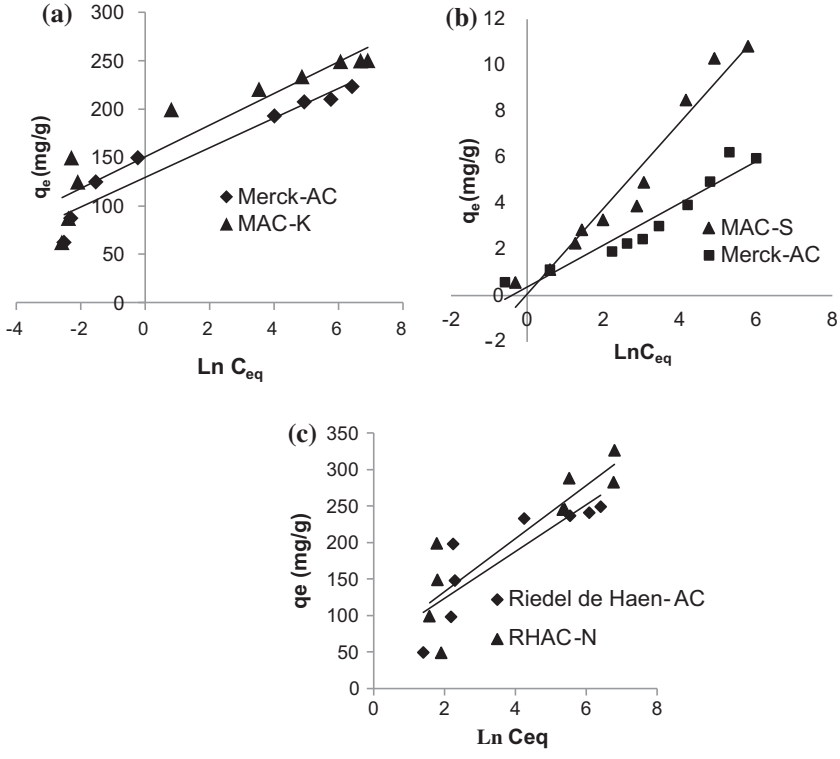

Fig. 8. Plots for Temkin adsorption isotherms of (a) Methylene blue, (b) Nickel, and (c) Bemacid blue on the functionalized activated carbons.

Table 5
Kinetic parameters for the adsorption of Ni^{2+}, methylene blue, and bemacid blue ET-L onto the functionalized activated carbons

Adsorbents	MAC-S		MAC-K		RHAC-N	
Pollutants	Ni^{2+}		Methylene blue		Bemacid blue ET-L	
Concentration (mg/g)	100	200	1,200	1,500	1,000	2,000
Pseudo-first-order						
$q_{e,exp}$ (mg/g)	2.48	5.23	149.99	187.48	245.37	260.87
$q_{e,calc}$ (mg/g)	4.98	1.00	58.55	2.16	76.83	124.59
k_1 (min^{-1})	3.24	0.99	1.49	1.59	2.19	2.19
R^2	0.87	0.94	0.85	0.90	0.85	0.86
Pseudo-second-order						
$q_{e,calc}$ (mg/g)	3.02	5.31	151.51	188.68	257.34	285.71
k_2 (g/mg/min)	2.03	2.55	109	2.81	2.01	0.01
h (mg/g/min) 10^{-3}	51.02	71.90	2.4 10^6	10^5	12 10^4	694.14
R^2	0.99	0.99	0.99	1.00	0.99	0.99
Intra-particle diffusion						
k_{int} (mg/g/$min^{0.5}$)	0.81	0.69	0.01	0.42	46.09	50.60
C (mg/g)	3.54	4.12	149.99	186.72	161.41	164.72
R^2	0.99	0.90	0.88	0.90	0.74	0.90

been used for this purpose. Transport of solute from the bulk of the solution to the outer surface of the film surrounding the particle-bulk transport, transport of solute within the film–film transport and transport in the interior of the particle or intra-particle transport are the main consecutive steps that usually occur in the adsorption process using a porous media.

$$q_t = k_{int} t^{0.5} + C \quad (9)$$

where K_{int} (mg g^{-1} $min^{-1/2}$) is the intra-particle diffusion rate constant and C (mg g^{-1}) is the intercept. The value of C gives an idea about the thickness of the boundary layer: the larger the intercept, the greater the boundary-layer effect.

Adsorption rate constants for Ni^{2+}, methylene blue, and bemacid blue ET-L were calculated using the three mentioned kinetics models represented by Eqs. (7)–(9), which were used to describe the adsorption mechanism. Even with relatively high values of R^2 (Table 5), the pseudo-first-order model was not well suited for describing the adsorption of all three pollutants used in this study since there is a difference between q_{exp} and q_{calc}. A relatively high R^2 values and close values of q_{exp} and q_{calc} indicate that pseudo-second-order model successfully describe the adsorption kinetics of all considered adsorbents as reported in Table 5. Weber's the intra-particle diffusion model Eq. (9) was used to elucidate the diffusion mechanism and to analyze the kinetic results. The plots q_t vs. $t^{1/2}$ (not shown) for two solute concentrations were used to calculate K_{int} from the slope and C parameters as reported in Table 5. It is seen that C parameter increased with increasing initial adsorbate concentration for up to 17.0% for Ni^{2+}, 24.5% for methylene blue and 3.4% for bemacid blue ET-L. The increase in the C values of all samples correspond to greater contribution in thickness of the boundary layer which lead to the greater the contribution of the surface sorption in the rate controlling step. The calculated k_{in} values are listed in Table 5. Since the linear plots (q_t vs. $t^{0.5}$) is of $y = ax + b$ form, indicating then, that the intra-particle diffusion was not only rate controlling step [45].

4. Conclusion

The ability of functionalized Merck and Riedel-de Haën commercial activated carbons to remove dyes and heavy metal ions from aqueous solutions has been investigated. This study showed that simple surface modifications using different chemical agents improve considerably their uptakes relative to the unfunctionalized states. Adsorption tests revealed the significant adsorptive capacity of functionalized MAC-K, MAC-S, and RACH-N, respectively, in the removal of methylene blue (12.5%), Ni^{2+} (83%), and bemacid blue ET-L (25%). The presence of surface functional groups, the pore structure, and the porosity-mesoporosity obtained by FTIR, SEM, and iodine number-methylene blue index, respectively, are important in adsorption experiments. The best fit to the experimental data was provided by Langmuir isotherm model. The adsorp-

tion kinetics for all three pollutants studied at different initial solutions concentrations and carbon loadings were best described using pseudo-second-order. This study shows that simple surface modifications of commercial activated carbons using chemical agents can enhance considerably their adsorptive properties in order to remove effectively dyes and heavy metals from aqueous solutions.

References

[1] Y. Akria, R.M. David, E. Philip, in: Proceedings of 21st Mid-Atlantic Industrial Waste Conference, Harrisburg, PA, June 26–27, Technomic, Lancaster, PA, USA, 1989.

[2] R. Perrin, J.P. Scharff, Chimie Industrielle (Industrial Chemistry), second ed., Dunod, Paris, 1999.

[3] S. Sirianuntapiboon, P. Srisornsak, Removal of disperse dyes from textile wastewater using bio-sludge, Bioresour. Technol. 98 (2007) 1057–1066.

[4] S.D. Khattri, M.K. Singh, Removal of malachite green from dye wastewater using neem sawdust by adsorption, J. Hazard. Mater. 167 (2009) 1089–1094.

[5] K.V.K. Rao, Inhibition of DNA synthesis in primary rat hepatocyte cultures by malachite green: a new liver tumor promoter, Toxicol. Lett. 81 (1995) 107–113.

[6] T. Robinson, G. McMullan, R. Marchant, P. Nigam, Remediation of dyes in textile effluent: A critical review on current treatment technologies with a proposed alternative, Bioresour. Technol. 77 (2001) 247–255.

[7] P.C.C. Faria, J.J. Órfão, M.F.R. Pereira, Adsorption of anionic and cationic dyes on activated carbons with different surface chemistries, Water Res 38(2004) 2043–2052.

[8] G. Mezohegyi, F.P. van der Zee, J. Font, A. Fortuny, A. Fabregat, A. Fabregat, Towards advanced aqueous dye removal processes: A short review on the versatile role of activated carbon, J. Environ. Manage. 102 (2012) 148–164.

[9] F.P. van der Zee, S. Villaverde, Combined anaerobic–aerobic treatment of azo dyes—A short review of bioreactor studies, Water. Res. 39 (2005) 1425–1440.

[10] N. Hidalgo, G. Mangiameli, T. Manzano, G.G. Zhadan, J.F. Kennedy, V.L. Shnyrov, M.G. Roig, Oxidation and removal of industrial textile dyes by a novel peroxidase extracted from post-harvest lentil (*Lens culinaris* L.) stubble, Biotechnol. Bioprocess Eng. 16 (2011) 821–829.

[11] Y. Fu, T. Viraraghavan, Fungal decolorization of dye wastewaters: A review, Bioresour. Technol. 79 (2001) 251–262.

[12] Q.S. Liu, T. Zheng, N. Li, P. Wang, G. Abulikemu, Modification of bamboo-based activated carbon using microwave radiation and its effects on the adsorption of methylene blue, Appl. Surf. Sci. 256 (2010) 3309–3315.

[13] D.O. Cooney, Adsorption Design for Wastewater Treatment, Lewis Publishers, Boca Raton, FL, 1999.

[14] S.A. Dastgheib, J. Ren, M. Rostam-Abadi, R. Chang, Preparation of functionalized and metal-impregnated activated carbon by a single-step activation method, Appl. Surf. Sci. 290 (2014) 92–101.

[15] W.T. Tsai, C.Y. Chang, S.Y. Wang, C.F. Chang, S.F. Chien, H.F. Sun, Preparation of activated carbons from corn cob catalyzed by potassium salts and subsequent gasification with CO2, Bioresour. Technol. 78 (2001) 203–208.

[16] A.P. Terzyk, The effect of carbon surface chemical composition on the adsorption of acetanilide, J. colloid interface sci. 272 (2004) 59–75.

[17] S. Saiful Azhar, A. Ghaniev Liew, D. Suhardv, K. Farizul Hafiz, M.D Irfan Hatim, Dye removal from aqueous solution by using adsorption on treated sugarcane bagasse, Am. J. Appl. Sci. 11 (2005) 1499–1503.

[18] ASTM, Standard Test Method for Determination of Iodine Number of Activated Carbon, ASTM Annual Book, 4 (1999) D 4607–94, Section 15.

[19] B. Bestani, N. Benderdouche, B. Benstaali, M. Belhakem, A. Addou, Methylene blue and iodine adsorption onto an activated desert plant, Bioresour. Technol. 99 (2008) 8441–8444.

[20] A. Ouldmoumna, L. Reinert, N. Benderdouche, B. Bestani, L. Duclaux, Characterization and application of three novel biosorbents "Eucalyptus globulus, Cynara cardunculus, and Prunus cerasefera" to dye removal, Desalin. Water Treat. 51 (2013) 3527–3538.

[21] L. Noszko, A. Bota, A. Simay, L. Nagy, Preparation of activated carbon from the by-products of agricultural Industry, Periodica Polytech. Chem. Eng. 28 (1984) 293–297.

[22] S. Attouti, B. Bestani, N. Benderdouche, L. Duclaux, Application of *Ulva lactuca* and *Systoceira stricta* algae-based activated carbons to hazardous cationic dyes removal from industrial effluents, Water Res. 47 (2013) 3375–3388.

[23] Y.S. Al-Degs, M.A.M. Khraisheh, S.J. Allen, N.A. Ahmad, Effect of carbon surface chemistry on the removal of reactive dyes from textile effluent, Water Res. 34 (2000) 927–935.

[24] P.C.C. Faria, J.J.M. Órfão, M.F.R. Pereira, Adsorption of anionic and cationic dyes on activated carbons with different surface chemistries, Water Res. 38 (2004) 2043–2052.

[25] J. Jaramillo, P.M. Álvarez, V.G. Serrano, Oxidation of activated carbon by dry and wet methods, Fuel Process. Technol. 91 (2010) 1768–1775.

[26] A. Duta, M. Visa, Simultaneous removal of two industrial dyes by adsorption and photocatalysis on a fly-ash–TiO_2 composite, J. Photochem. Photobiol., A 306 (2015) 21–30.

[27] Y.S. Aldegs, M. Elbarghouthi, A.H. Elsheikh, G.M. Walker, Effect of solution pH, ionic strength, and temperature on adsorption behavior of reactive dyes on activated carbon, Dyes Pigm. 77 (2008) 16–23.

[28] F. Nemchi, B. Bestani, N. Benderdouche, M. Belhakem, L.C. de Minorval, Adsorption of Supranol yellow 4GL from aqueous solution onto activated carbons prepared from seawater algae, Adsorpt. Sci. Technol. 30 (2012) 81–96.

[29] N. Benderdouche, B. Bestani, B. Benstaali, Z. Derriche, Enhancement of the adsorptive properties of a desert *Salsola vermiculata* species, J. Adsorpt. Sci. Technol. 21 (8) (2003) 739–750.

[30] M. Kobya, E. Demirbas, E. Senturk, M. Ince, Adsorption of heavy metal ions from aqueous solutions by activated carbon prepared from apricot stone, Bioresour. Technol. 96 (2005) 1518–1521.
[31] N. Petrov, T. Budinova, I. Khavesov, Adsorption of the ions of zinc, cadmium, copper, and lead on oxidized anthracite, Carbon 30 (1992) 135–139.
[32] M. Sassi, B. Bestani, A. Hadj Said, B. Benderdouche, E. Guibal, Removal of heavy metal ions from aqueous solutions by a local dairy sludge as a biosorbent, Desalination 262 (2010) 243–250.
[33] N. Thinakaran, P. Baskaralingam, M. Pulikesi, P. Panneerselvam, S. Sivanesan, Removal of acid violet 17 from aqueous solutions by adsorption onto activated carbon prepared from sunflower seed hull, J. Hazard. Mater. 151 (2008) 316–322.
[34] G. Crini, H.N. Peindy, F. Gimbert, C. Robert, Removal of C.I. basic green 4 (malachite green) from aqueous solutions by adsorption using cyclodextrin-based adsorbent: Kinetic and equilibrium studies, Sep. Purif. Technol. 53 (2007) 97–110.
[35] M.J. Temkin, V. Pyzhev, Kinetics of ammonia synthesis on promoted iron catalysts, Acta Physiochim., Urs. 12 (1940) 217–222.
[36] N. Ouslimani, M. Maallem, Adsorption of dyes yellow Bemacid CM-3R and red Bemacid CL-BN200 by a solid bentonite, Int. Sci. J. Altern. Energy Ecol. 62 (2008) 219–223
[37] S.K. Theydan, M.J. Ahmed, Adsorption of methylene blue onto biomass-based activated carbon by $FeCl_3$ activation: Equilibrium, kinetics, and thermodynamic studies, J. Anal. Appl. Pyrolysis 97 (2012) 116–122.
[38] H. Parab, S. Joshi, N. Shenov, A. Lali, U.S. Sarmat, M. Sudernan, Determination of kinetic and equilibrium parameters of the batch adsorption of Co(II), Cr(III) and Ni(II) onto coir pith, Process Chem. 41 (2005) 609–615.
[39] Longzhe Cui, G. Wu, Tae-seop Jeong, Adsorption performance of nickel and cadmium ions onto brewer's yeast, Can. J. Chem. Eng. 88 (2010) 109–115.
[40] F. Gönen, D.S. Serin, Adsorption study on orange peel: Removal of Ni(II) ions from aqueous solution, Afr. J. Biotechnol. 11 (2012) 1250–1258.
[41] H. Benaïssa, A. Benaïssa, Z. Senouci-Berekci, Feasibility study of acid dye removal from synthetic aqueous solutions by sorption using two varieties of orange peel in batch mode, http://www.uest.gr/win4life/images/papers/benaissa1.pdf
[42] Y.S. Ho, G. McKay, Pseudo-second order model for sorption processes, Process Biochem. 34 (1999) 451–465.
[43] S. Lagergren, Zur theorie der sogenannten adsorption geloester stoffe, Kungliga Svenska Vetenskapsakademiens, Handlingar 24 (1898) 1–39.
[44] W.J. Weber, J.C. Morris, Kinetics of adsorption on carbon from solution, J. Sanit. Eng. Div. Am. Soc. Civ. Eng. 89 (1963) 31–60.
[45] F.C. Wu, R.L. Tseng, R.S. Juang, Initial behavior of intraparticle diffusion model used in the description of adsorption kinetics, Chem. Eng. J. 153 (2009) 1–8.